

Superabsorption of light by nanoparticles

Konstantin Ladutenko*

*ITMO University, 49 Kronverskii Ave., St. Petersburg 197101, Russian Federation and
Ioffe Physical-Technical Institute of the Russian Academy of Sciences,
26 Polytekhnicheskaya Str., St. Petersburg 194021, Russian Federation*

Pavel Belov

ITMO University, 49 Kronverskii Ave., St. Petersburg 197101, Russian Federation

Ovidio Peña-Rodríguez

*Instituto de Fusión Nuclear, Universidad Politécnica de Madrid,
José Gutiérrez Abascal 2, E-28006 Madrid, Spain*

Ali Mirzaei, Andrey Miroschnichenko, and Ilya Shadrivov

*Nonlinear Physics Centre, Research School of Physics and Engineering,
The Australian National University, 59 Mills Rd, Acton, ACT, 2601, Australia
(Dated: July 17, 2015)*

Nanoparticles have a fundamental limit as to how much light they can absorb. This limit is based on the finite number of modes excited in the nanoparticle at a given wavelength and maximum absorption capacity per mode. The enhanced absorption can be achieved when each mode supported by the nanoparticle absorbs light up to the maximum capacity. Using stochastic optimization algorithm, we design multilayer nanoparticles, in which we can make several resonant modes overlap at the same frequency resulting in *superabsorption*. We further introduce the *efficiency of the absorption* for a nanoparticle, which is the absorption normalized by the physical size of the particle, and show that efficient absorbers are not always operating in the superabsorbing regime.

PACS numbers: 41.20.Jb 42.25.Bs 02.60.Pn 02.70.-c

Mie theory [1], which is over 100 years old, describes interaction of electromagnetic waves with spherical particles. Mie solution is still of great interest these days [2–8], since it is one of the primary tools for analyzing wave scattering by spherical objects. Further development of the Mie theory [9, 10] made it possible to apply it to the study of multilayer spherical particles [11, 12]. Such particles have various applications in cancer treatment [13, 14], medical diagnostics [15], cloaking [16–18] and plasmonic devices [19, 20], in the study of thermal properties of insulating materials [21], as well as for improving solar cells performance [22, 23].

The scattering properties of multilayer cylinders and spheres was studied in great detail by Ruan and Fan [24, 25]. In these works the authors introduced the concept of superscattering, when scattering cross-section of a multilayer particle exceeds that of a homogeneous particle of the same size in the so-called single-channel limit. Superscattering appears when a multilayer structure has several nearly degenerate modes, i.e. their resonance frequencies coincide or are close to each other. In a homogeneous particle, resonances appear at different frequencies, and there is no design freedom to make these resonances overlap, and this limits the achievable scattering cross-section.

Similar fundamental limitations exist for the absorbing properties of subwavelength nanoparticles. Tribelsky [26] has derived a theoretical limit of a maximum

absorption cross-section (ACS) value for a single channel, i.e., when only one mode of a sphere is excited. As a result, the absorption coefficients $\tilde{a}_n = \text{Re}\{a_n\} - |a_n|^2$ and $\tilde{b}_n = \text{Re}\{b_n\} - |b_n|^2$ become limited by 1/4, here a_n and b_n are scattering coefficient as defined within the Mie theory [27].

To overcome these limitations, we employ similar approach to the one used for enhancing scattering cross-section [25]. In particular, we propose to use the multilayer structures, and by means of stochastic optimization algorithm we optimize the ACS of such nanoparticles. We analyze the absorption cross-section of these particles, and present the superabsorption regime. We further introduce the absorption efficiency, which is the ACS normalized to the geometric cross-section of particles. Here we show that there is a strong counterplay between the increased absorption for larger particles vs size for smaller particles, and quite remarkably we find that the most *efficient* absorption can be achieved in a single channel limit for small particles.

Another approach for an ideal absorber is given in the recent work by Grigoriev et al. [28]. Authors considered only dipole approximation, and the final result is very close to the dipole limit predicted by Tribelsky [26]. Such absorption design corresponds to the single mode limit. At the same time, Grigoriev et al. [28] also provide an equation to design a core-shell structure from given materials. However, in the case of *Si* core and *Ag* shell mate-

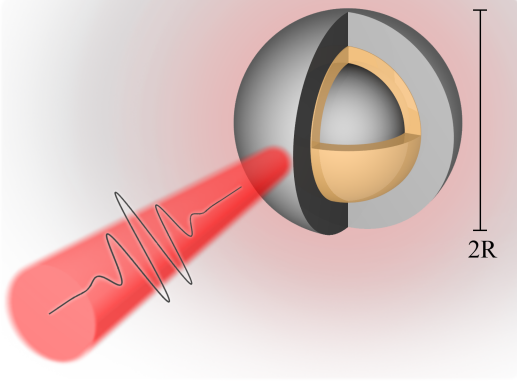


Figure 1. Schematic view of the simulated *Si/Ag/Si* particle.

materials and sizes taken from the best design obtained in the present paper, their equation gives a complex value for the core material filling factor, which cannot be achieved in experimental realisations.

We start our analyses by considering the triple-layer *Si/Ag/Si* spherical particle illuminated with a plane wave schematically shown in Fig. 1. In what follows we describe the materials using experimentally measured parameters from Ref. [29], and, e.g. at $\lambda = 500$ nm $\epsilon_{Si} = 18.5 + i0.63$ and $\epsilon_{Ag} = -8.5 + i0.76$. To optimize the thickness of each layer we implemented [30] an adaptive differential evolution algorithm [31], which is called JADE [32]. The technical details of the optimization algorithm were published previously in Ref. [18]. We perform Mie calculations using the Scatttnlay software [10, 33], whose results are verified by a number of other implementations of the Mie solutions and by commercially available software including CST Microwave studio [34] and Comsol Multiphysics [35].

It is a common understanding that, in general, a larger particle has a larger absorption cross-section, so sphere with the diameter of 1 cm absorbs more light than any nanoscale sphere. Therefore, it is practical to employ the *absorption efficiency* $Q_{\text{abs}} = C_{\text{abs}}/\pi R^2$, where R is the outer radius of the particle and C_{abs} is the absorption cross-section.

In order to study the dependence of the absorption efficiency on the outer particle size, we run optimization algorithm for different (fixed) particle outer size, and our optimization parameters are the radii of internal cores, whereas the target function is the absorption efficiency. We maximize absorption efficiency at a fixed wavelength of the incident light (we have chosen $\lambda = 500$ nm). We show the results of our stochastic optimization algorithm in Fig. 2 (a). Dashed lines show theoretical absorption limit of a dipole ($n = 1$) and a quadrupole ($n = 2$) reso-

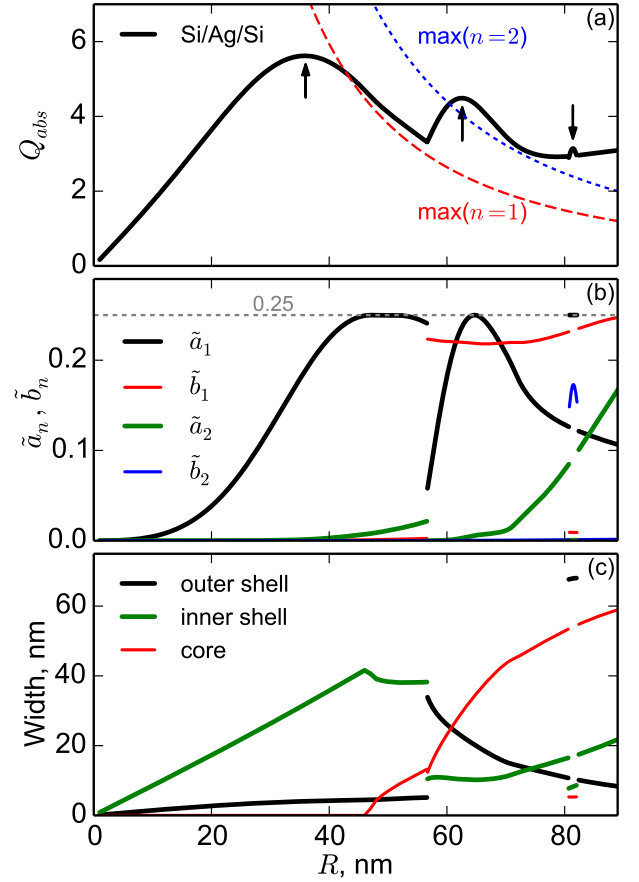


Figure 2. Results of optimization of the absorption efficiency for the fixed wavelength of 500 nm. (a) Absorption efficiency with the best value achieved for the particle of the radius of 36 nm and Ag/Si design (zero sized core). Dashed lines show theoretical limits for the first channel and second channel absorption. The second and third peaks in the absorption efficiency curve exceed the theoretical limit for the second mode absorption at $R = 63$ nm and $R = 81$ nm. Local maxima of absorption efficiency are additionally marked with arrows. (b) Mie absorption coefficients for individual excited modes of the optimized structures. (c) Optimized layer thicknesses. For the total particle radius below 46 nm the optimizer converges to a bi-layer structure, when core size vanishes, and the optimum design is a *Ag/Si* particle.

nances [26], which are given as

$$Q_{\text{abs max}}^{(n)} = \frac{2n+1}{2q^2},$$

where the size parameter $q = 2\pi R/\lambda$, and n is the angular momentum of the mode. Following Ref. [25], where the authors introduce superscattering for spherical particles, here we introduce superabsorption regime, when the ACS is larger than the theoretical limit for absorption by the mode with the highest excited angular momentum n . In our parameter space we have just modes up to the quadrupole excited ($n = 2$), and in order to get superabsorption our efficiency should be higher than that of a

quadrupole. We clearly see this superabsorption regime at $R > 60$ nm, in Fig. 2 (a).

In Fig. 2 (b) we present the values of Mie absorption coefficients for individual excited modes in the structure, while horizontal dashed line shows the theoretical limit ($1/4$) for each of them. $\tilde{a}_{1,2}$ are electric dipole and electric quadrupole, while $\tilde{b}_{1,2}$ are magnetic dipole and magnetic quadrupole. For small particles, as expected, absorption is dominated by electric dipole \tilde{a}_1 . At $R > 56.6$ nm the optimization procedure finds that the designs with both electric and magnetic dipoles have larger ACS than the structure with only the electric dipole excited. This is why the curves in Figs. 2 (b,c) experience the discontinuity. We also note that there is a very narrow range of particle sizes, between 80.7 nm and 82.1 nm, where our analysis finds that the design supporting electric dipole \tilde{a}_1 and magnetic quadrupole \tilde{b}_2 has larger ACS, and this explains two more discontinuities of the curves at the respective size values.

Fig. 2 (c) shows optimized sizes of layers inside a multilayer structure. It reveals quite a curious result, that the dipole branch (i.e. for particle radii below 56.6 nm) has two parts. For $R < 46$ nm the best absorber has just two layers, as the radius of the core of a triple-layer structure vanishes, and the particle reduces to *Ag/Si* core-shell structure. At $R = 46$ nm dipole channel reaches its theoretical limit (it becomes $\tilde{a}_1 > 0.249$). It appears that the optimizer introduced the inner *Si* layer in order to keep \tilde{a}_1 near the theoretical limit as the R increases. As a side effect, the quadrupole contribution \tilde{a}_2 appears; however, it does not help to reach superabsorption limit for $n = 2$.

Remarkably, the absolute maximum *absorption efficiency* is not reached within the superabsorption regime. Figure 2 shows that the maximum efficiency is achieved for small particle size, and the ACS is still well below the single channel limit. It appears that the *Ag/Si* core-shell nanoparticle with the total radii of approximately 36 nm is the most efficient absorber among the considered structures, whose ACS reaches values *over 5 times the physical cross-section area of the particle*. From a practical point of view, it is quite important that the maximum can be reached in a bi-layer structure, instead of a triple-layer, since it should be easier and cheaper to fabricate.

To study spectral properties of structures with large ACS which we obtained by the optimization, in Fig. 3 we plot three different cases for designs that correspond to local maxima of Q_{abs} shown in Fig. 2 (a). As expected, the design corresponding to the maximum absorption efficiency at $R = 36$ nm has a single electric dipole resonance centered at the target wavelength $\lambda = 500$ nm. Spectra of designs with maxima at $R = 63$ nm and $R = 81$ nm have a signature of the superabsorption, i.e. there is an overlap of several resonances. We note that these structures have additional absorption resonances, but they are located far from the wavelength of interest. A noticeable feature of Fig. 3 (c) is an almost flat top

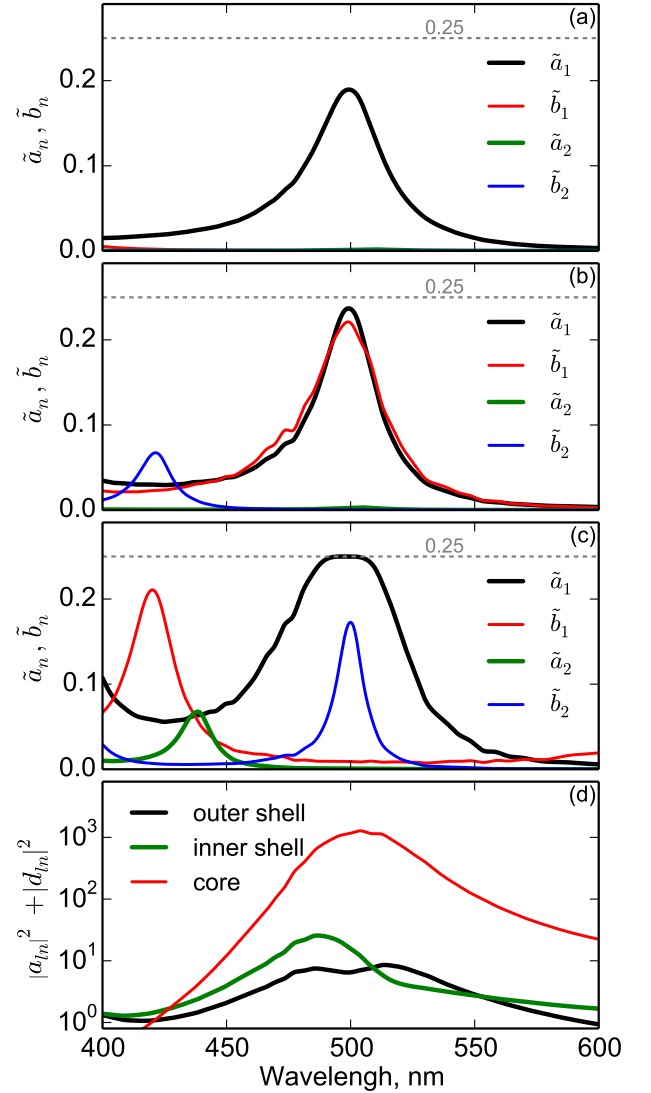


Figure 3. Spectra of Mie absorption coefficients of (a) efficient and (b-c) superabsorption design. Panel (d) shows the superposition of the squared absolute values of the Mie coefficients for electric dipole contribution inside each layer.

of the electric dipole resonance. More detailed analysis shows that we have *excited several electric dipole resonances* with close resonance frequencies within our multilayer structure. Indeed, if we plot a superposition of the squares of the absolute values of the Mie coefficients, which characterize energy stored in each layer, we find that we excite resonances in all three layers, and they are slightly offset as shown in Fig. 3 (d). Combined effect of these resonances produces the flat and relatively broadband electric resonance response shown in Fig. 3 (c).

Finally, we present distribution of the amplitude of the electric field in Fig. 4 for two designs: with the best efficiency at $R = 36$ nm and in a superabsorbing design with $R = 63$ nm. Using semi-transparent white curves we also plot streamlines of the Poynting vector which character-

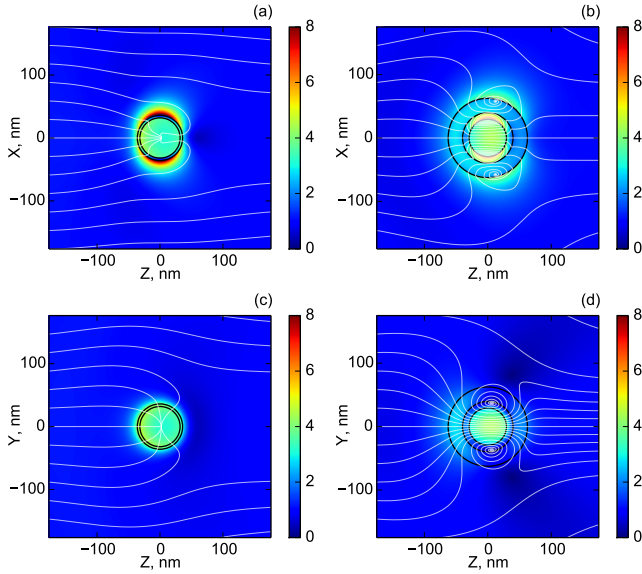


Figure 4. Amplitude of electric field for $R = 36$ nm (a,c) and superabsorbing designs (b,d) in E-k (a-b) and H-k (c-d) planes normalized to incident wave.

ize energy flow. For the effective design of the absorber, the power from a large cross-sectional area flows into the particle. In case of superabsorption regime, we observe the formation of vortices in the power flow, which make absorption more efficient as the electromagnetic energy propagates several times through the absorbing materials. The reason for the smaller overall absorption efficiency of a superabsorbing design is obvious: spatial distribution of the electric field is not uniform inside the particle and the share of the volume with high absorption rate in the vortices does not compensate low absorption efficiency in the regions with small electric field (absorbed power is expressed as $P_{\text{abs}} = \frac{1}{2} \int \sigma |E|^2 dx dy dz$)

In conclusion, we introduce and study the effect of superabsorption, when the absorption cross-section of the nanoparticle can reach the theoretical limit for several modes at the same frequency. This becomes possible when several resonant modes of the structure overlap at the same frequency, and this regime can be achieved in multilayer nanoparticles. Moreover, quite unexpectedly we find that the most efficient absorbers, which are characterized by enhanced absorption efficiencies, are smaller nanoparticles working in a single mode regime. We present their spectral characteristics and field structure. The stochastic algorithm utilized in our approach is very generic and the optimization can be repeated for any desired wavelength or wavelength range. As a result, one can design spectrally-selective absorbers or broadband absorbers with almost arbitrary prescribed properties. It is interesting to note that a similar conclusion was made by Miller et al. [36] for extinction of arbitrary particles: small size with only dipole response is preferable

for geometric volume normalized efficiency.

Thanks to David A. Powell for his contribution to the analysis of the spectrum feature. AEM and IVS would like to acknowledge support from the Australian Research Council through Future Fellow and Discovery project schemes. KSL and PAB would like to thank the Ministry of Education and Science of the Russian Federation and Government of the Russian Federation (Grant 074-U01) for the financial support.

* e-mail: k.ladutenko@metalab.ifmo.ru

- [1] G. Mie, *Annalen der Physik* **330**, 377 (1908).
- [2] H. Suzuki and I.-Y. S. Lee, *International Journal of Physical Sciences* **3**, 038 (2008).
- [3] D. MacKowski, *Springer Series in Optical Sciences* **169**, 223 (2012).
- [4] J. Lermé, *The European Physical Journal D - Atomic, Molecular, Optical and Plasma Physics* **10**, 265 (2000).
- [5] H. Xu, *Phys. Rev. B* **72**, 073405 (2005).
- [6] R. Li, X. Han, H. Jiang, and K. F. Ren, *Appl. Opt.* **45**, 1260 (2006).
- [7] A. Gogoi, A. Choudhury, and G. Ahmed, *Journal of Modern Optics* **57**, 2192 (2010).
- [8] M. A. Santiago-Cordoba, S. V. Boriskina, F. Vollmer, and M. C. Demirel, *Applied Physics Letters* **99**, 073701 (2011).
- [9] W. Yang, *Applied Optics* **42**, 1710 (2003).
- [10] O. Peña and U. Pal, *Computer Physics Communications* **180**, 2348 (2009).
- [11] S. W. Sheehan, H. Noh, G. W. Brudvig, H. Cao, and C. A. Schmuttenmaer, *The Journal of Physical Chemistry C* **117**, 927 (2013).
- [12] M. Selmke, M. Braun, and F. Cichos, *ACS Nano* **6**, 2741 (2012).
- [13] J. Zhang, *Journal of Physical Chemistry Letters* **1**, 686 (2010).
- [14] L. Hirsch, R. Stafford, J. Bankson, S. Sershen, B. Rivera, R. Price, J. Hazle, N. Halas, and J. West, *Proceedings of the National Academy of Sciences of the United States of America* **100**, 13549 (2003).
- [15] L. R. Allain and T. Vo-Dinh, *Analytica Chimica Acta* **469**, 149 (2002).
- [16] C.-W. Qiu, L. Hu, X. Xu, and Y. Feng, *Phys. Rev. E* **79**, 047602 (2009).
- [17] X. Wang, F. Chen, and E. Semouchkina, *AIP Advances* **3**, 112111 (2013).
- [18] K. Ladutenko, O. Peña Rodríguez, I. Melchakova, I. Yagupov, and P. Belov, *Journal of Applied Physics* **116**, 184508 (2014).
- [19] J. Martin, J. Proust, D. Grard, and J. Plain, *Optical Materials Express* **3**, 954 (2013).
- [20] A. Alu and N. Engheta, *Phys. Rev. E* **72**, 016623 (2005).
- [21] T. Xie, Y.-L. He, and Z.-J. Hu, *International Journal of Heat and Mass Transfer* **58**, 540 (2013).
- [22] Y. Kameya and K. Hanamura, *Solar Energy* **85**, 299 (2011).
- [23] S. A. Mann, R. R. Grote, R. M. Osgood, and J. A. Schuller, *Opt. Express* **19**, 25729 (2011).
- [24] Z. Ruan and S. Fan, *Phys. Rev. Lett.* **105**, 013901 (2010).

- [25] Z. Ruan and S. Fan, Applied Physics Letters **98**, 043101 (2011).
- [26] M. I. Tribelsky, EPL (Europhysics Letters) **94**, 14004 (2011).
- [27] C. F. Bohren and D. Huffman, *Absorption and scattering of light by small particles*, Wiley science paperback series (Wiley, 1983).
- [28] V. Grigoriev, N. Bonod, J. Wenger, and B. Stout, ACS Photonics **2**, 263 (2015), <http://dx.doi.org/10.1021/ph500456w>.
- [29] E. Palik, *Handbook of Optical Constants of Solids, Five-Volume Set: Handbook of Thermo-Optic Coefficients of Optical Materials with Applications* (Elsevier Science, 1997).
- [30] <https://github.com/kostyfisik/jade>.
- [31] R. Storn and K. Price, Journal of Global Optimization **11**, 341 (1997).
- [32] J. Zhang and A. Sanderson, Evolutionary Computation, IEEE Transactions on **13**, 945 (2009).
- [33] <https://github.com/ovidioppr/scattnlay>.
- [34] <https://www.cst.com/Products/CSTMWS>.
- [35] <http://www.comsol.com/comsol-multiphysics>.
- [36] O. D. Miller, C. W. Hsu, M. T. H. Reid, W. Qiu, B. G. DeLacy, J. D. Joannopoulos, M. Soljačić, and S. G. Johnson, Phys. Rev. Lett. **112**, 123903 (2014).